HATSOPOULOS MICROFLUIDS LABORATORY
Department of Mechanical Engineering, Massachusetts Institute of Technology

Ex vivo Rheology of Spider Silk

N. Kojic, J. Bico, C. Clasen, & G. H. McKinley

August 5, 2005
HML Report Number 05-P-08

HML@MIT
http://web.mit.edu/fluids

Ex vivo rheology of spider silk

N. Kojić[1,2], J. Bico[1,3], C. Clasen[4] & G. H. McKinley[1]

[1]*Hatsopoulos Microfluids Laboratory, Department of Mechanical Engineering, MIT,*

[2]*Harvard-MIT Division of Health Sciences and Technology,*

Cambridge, Massachusetts 02139, USA.

[3]*PMMH-ESPCI, CNRS UMR 7636, 75231 Paris Cedex 05, France.*

[4]*Institut für Technische und Makromolekulare Chemie, 20146 Hamburg, Germany.*

Submitted to *Proceedings of the Royal Society B*

Abstract

We investigate the rheological properties of microliter quantities of the spinning material extracted *ex vivo* from the major ampullate gland of a *Nephila clavipes* spider using two new micro-rheometric devices. A sliding plate micro-rheometer is employed to measure the steady-state shear viscosity of ~1μL samples of silk dope from individual biological specimens. The steady shear viscosity of the spinning solution is found to be highly shear-thinning with a power-law index consistent with values expected for liquid crystalline solutions. Calculations show that the viscosity of the fluid decreases ten-fold as it flows through the narrow spinning canals of the spider. By contrast, measurements in a microcapillary extensional rheometer show that the transient extensional viscosity (i.e. the viscoelastic resistance to stretching) of the spinning fluid increases more than one hundred-fold during the spinning process. Quantifying the properties of native spinning solutions provides new guidance for adjusting the spinning processes of synthetic or genetically-engineered silks to match those of the spider.

Keywords: silk rheology, Nephila clavipes, microrheometry, extensional viscosity

1. Introduction

Over the past decade numerous studies have shown that spider dragline silk has a number of unique material properties (Becker *et al.* 2003; Gosline *et al.* 1999; Shao and Vollrath 2002), yet how exactly the spider processes its fibre remains unclear. Recent experiments with recombinant spider silk (Lazaris *et al.* 2002) and other studies performed with silkworms (Shao and Vollrath 2002) show that careful control of the processing conditions for fibre spinning is key to obtaining superior mechanical properties in spun silks. Forced silking at different rates results in modified kinematics in the spinning canal and substantial changes in the mechanical properties of the resulting silk fibres (Perez-Rigueiro *et al.* 2005). To understand this complex flow process it is essential to elucidate the rheological properties of the initial liquid spinning material, commonly referred to as "spinning dope" (Vollrath and Knight 2001) that is stored in the spinning glands of the spider (Chen *et al.* 2002). Although the spinning dope is a concentrated aqueous solution containing 25-30 wt.% protein, all rheological experiments to date have been performed with diluted solutions (typically <5 wt.% of protein) (Chen *et al.* 2002).

Recently, processing experiments have been performed with reconstituted silk solutions obtained from the silkworm *Bombyx mori* (Jin and Kaplan 2003). Micellar solutions with ~8 wt% silk were reconstituted using dialysis. However in order to produce spinnable fibres, a high molecular weight linear polymer (polyethylene oxide with molecular weight of 0.9×10^6 g/mol) was added to the reconstituted solutions. This additional component augments the 'spinnability' of the dope by increasing extensional or 'tensile' viscosity of the fluid and prevents capillary break-up of the fluid jet. The resulting

spun fibres exhibited morphological features, such as increased birefringence and alignment, similar to the native silk fibre. These experiments suggest that native silk solutions possess significant non-Newtonian fluid properties (Chen *et al.* 2002; Terry *et al.* 2004), however more insight would be gained through direct rheological characterisation of the native, concentrated spider silk dope.

Recently published results (Terry *et al.* 2004) of bulk shear rheometry on larger scale samples of silkworm silk solutions indicate strong viscoelastic properties for silk dope with a zero-shear-rate viscosity on the order of 10^3 Pa.s and a critical rate of the onset of shear thinning on the order of 1 s^{-1}. Phase separation and unstable flow conditions above this critical rate were interpreted as indication for a shear-induced beta-sheet formation.

The volume of spinning dope that can be harvested from a single major ampullate gland of *N. clavipes* is approximately 5 – 10 µl. Besides the minute quantity available, the dope is viscous (Willcox *et al.* 1996) and tends to dry with time, making it difficult to obtain reliable viscometric data. Many of these difficulties can be overcome by using micro-rheometry. The majority of micro-rheometric techniques available for the characterization of complex biofluids rely on Brownian forcing of microscopic tracer beads. The rheological properties of the surrounding fluid matrix are obtained from the time-correlated displacement of the bead via a deconvolution process (Mukhopadhyay and Granick 2001; Solomon and Lu 2001). Such techniques are inherently limited to studies of linear viscoelastic properties of the test fluid at small shearing strains. By contrast, the silk spinning process involves large strains and both shearing and extensional kinematic components (Knight and Vollrath 1999). It is these large deformations that lead to

development of non-equilibrium texture morphologies in the spun silk (Vollrath and Knight 2001). In order to address these issues, two new micro-rheometric instruments have been constructed: a flexure-based micro-rheometer (Clasen and McKinley 2004; Gearing and Anand 2001) for steady and oscillatory shearing measurements and a capillary breakup micro-rheometer for extensional rheometry (Bazilevsky *et al.* 1990; McKinley and Tripathi 2000).

Here we describe the application of these instruments in measuring the rheological properties of dragline silk solutions extracted from the major ampullate gland of *Nephila* spiders.

2. Materials and Methods

Both of the experimental devices utilized in the present study have been specifically designed to accommodate the small quantities (~1μL) of fluid available from a single major ampullate gland of the *Nephila clavipes* spider as shown in figure 1. Thus, these micro-rheometric devices enable *ex vivo* testing of the native spinning dope from which the spider spins dragline and web frame fibres (Gosline *et al.* 1999; Vollrath and Knight 2001).

Dissections were performed using a standard dissecting scope and the ampullate glands were extracted and stored under distilled water for less than 5 minutes whilst being transferred to the micro-rheometers for testing. Each sample was only utilized once due to progressive evaporation of the aqueous phase to the environment.

The flexure-based micro-rheometer generates a plane Couette shearing flow between two plates that are aligned using white light interferometry and separated by a precisely-controlled gap of 1–150 μm (figure 2*a*). The plates consist of cylindrical optical flats that are then diamond-machined to provide the required rectangular test surface area. The shear stress exerted on the sample (ranging from 2 to 10^4 Pa) is calculated from the deflection of the upper flexure as the lower one is actuated. The imposed shear rate, defined as the ratio of the actuated plate velocity and the inter-plate gap, $\dot{\gamma} = V / h$, can be varied over the range $2\times10^{-4} < \dot{\gamma} < 4\times10^{2}$ s^{-1}. Further details of the instrumentation are provided elsewhere (Clasen and McKinley 2004; Clasen and McKinley 2005 submitted).

Recently it has been noted that the converging flow in the duct of the major ampullate gland has significant extensional kinematics that can lead to pronounced molecular extension and orientation (Knight and Vollrath 1999; Vollrath and Knight 2001). If macroscopic volumes of the entangled polymer solution are available then the extensional viscosity of a viscous liquid can now be measured reliably using filament stretching rheometry (Bhattacharjee *et al.* 2002). However, given the limited amount of raw dope available, this method becomes impractical. In the present work we have developed a microscale capillary break-up extensional rheometer to measure the transient extensional viscosity η_e (McKinley and Tripathi 2000). The experimental procedure involves placing a drop of the spinning dope in between two cylindrical endplates of radius R_p = 1.5mm. The plates are then pulled apart to a distance of 5 mm in order to impose a step axial strain on the sample and form a liquid thread (figure 3). The instrument can be placed in an environmental chamber to control test temperature and relative humidity if desired;

however the present tests were all performed in standard laboratory environment (T = 22˚C, relative humidity 25-35%). The viscoelastic fluid column that is formed by the step extensional strain subsequently thins under the action of capillarity, while viscous and elastic forces tend to impede the necking process. The time rate of change of the liquid filament is monitored using a laser micrometer with a resolution of ± 10 μm (Omron model ZL4A). Gravitational drainage is not important for such small samples, and the filament evolves in a self-similar manner. It has been shown that the apparent extensional viscosity function can be deduced from the self-similar thinning and pinch-off dynamics of the viscous fluid thread (McKinley and Tripathi 2000) via the expression

$$\eta_e = -0.213 \frac{\sigma}{dR/dt}. \qquad (2.1)$$

Here σ is the surface tension of the liquid, *R(t)* is the midpoint radius of the thread measured with the laser micrometer, and the numerical prefactor is derived from a slender-body lubrication theory for a viscous incompressible Newtonian fluid in order to account for deviations from a purely cylindrical geometry in the vicinity of the endplates (McKinley and Tripathi 2000).

Due to the high viscosity of the silk and the evaporation of the aqueous solvent it was not possible to directly measure the surface tension of the silk. We therefore select as an appropriate value, $\sigma \approx 60 \times 10^{-3} N/m$ which agrees with measured values for other aqueous polymer solutions (Adamson and Gast 1997; Christanti and Walker 2001; Cooper-White *et al.* 2002).

3. Results

(a) Shear Viscosity of *Ex vivo* Silk Solutions

The sliding plate micro-rheometer was used to measure the shear-rate-dependence of the steady shear viscosity $\eta(\dot{\gamma})$ for a ~1 μL blob of spinning dope extracted from the major ampullate gland. The dope was sheared between two 25 mm^2 optical plates with the gap set to 25 μm (figure 2*a*). In the limit of zero shear rate, the data in figure 2*b* shows that the viscosity of the spinning dope is $\eta_0 = 3500$ Pa.s (or 3.5×10^6 times the viscosity of water). However, under stronger deformation rates the dope viscosity drops significantly with increasing shear rate, i.e. the dope has a shear-thinning viscosity (figure 2*b*). This effect is characteristic of concentrated polymer solutions due to the loss of molecular entanglements and can be described by molecular theories or by phenomenological constitutive models such as the Carreau-Yasuda equation (Bird *et al.* 1987; Yasuda *et al.* 1981):

$$\eta = \eta_0[1 + (\dot{\gamma}\lambda)^a]^{(n-1)/a}, \qquad (3.1)$$

where λ is a measure of the relaxation time of the viscoelastic fluid (its inverse is the critical shear rate that marks the onset of shear thinning), n is the power-law exponent characterizing the shear-thinning regime observed at high shear rates, and the coefficient a describes the rate of transition between the zero-shear-rate region and the power-law region.

The adjustment of these parameters to our data yields values of $\lambda = 0.40$ s, $a = 0.68$ and $n = 0.18$, which are characteristic for a strongly shear-thinning fluid (Yasuda *et al.*

1981). A comparison to shear rheological data for *B. mori* dope determined with the same experimental setup and shown in figure 2*b* gives comparable viscoelastic properties for silk dope from the silkworm and the spider. The constitutive parameters obtained are tabulated in table 1. The observed shear-thinning behaviour for the silkworm dope is in good agreement with recent experiments performed with a commercial rheometer (Terry *et al.* 2004), in which the zero-shear viscosity measured was about 2 kPa.s (we measured 5 ± 1 kPa.s) and the critical shear-rate above which shear-thinning occurs was of order 0.5 s^{-1} (we determined 1.7 s^{-1}).

(b) Extensional Rheology

The data in figure 3*b* shows that at small strains the extensional viscosity η_e is three times larger than the zero-shear-rate viscosity measured with the shearing micro-rheometer. This observation is consistent with the classical results of Trouton for a Newtonian liquid (Trouton 1906). However, at large strains the necking dynamics are greatly retarded as the filament simultaneously strain hardens and undergoes mass transfer to the surroundings (i.e. evaporative drying). This strain-hardening stabilizes the spinline and leads to the formation of axially-uniform filaments (Olagunju 1999). The apparent extensional viscosity therefore diverges and the thinning fluid thread ultimately dries to become a solid filament with a fixed finite radius. In contrast to an actual dragline filament which is spun under a constant force corresponding to the weight of a spider (Gosline *et al.* 1999), in our capillary break-up device there is no externally-imposed tension. The final thread radius is measured to be $R_f \approx 20$ μm. The solid lines in figure 3*a* correspond to a one-dimensional model of this drying process which is discussed in detail below.

4. Discussion

The strong shear-rate dependence of the silk viscosity shown in figure 2 is of considerable importance during extrusion. During a typical spinning process (Shao and Vollrath 2002; Vollrath and Knight 2001), the *Nephila* spider draws out a 4 μm diameter thread at a speed of 20 mm/s corresponding to a flow rate of Q = 0.25 nL/s. We approximate the geometry of the long converging spinning canal (or *S-duct)* shown in figure 1*b* as a truncated cone of length L = 20 mm, and with maximum/minimum diameters of D = 200 μm and d = 4 μm respectively. For the given geometry and flow rate, the pressure drop associated with steady flow of a viscous shear-thinning dope through the canal can be estimated from hydrodynamic lubrication theory (Bird *et al.* 1987 eq. 4.2-10), which leads to the following expression for the relative pressure drop for steady flow of a power-law liquid through a linearly tapered tube compared to that expected for a Newtonian fluid:

$$\frac{\Delta P_{silk}}{\Delta P_{Newtonian}} = \frac{2^{3(n-1)}\,\lambda^{n-1}}{4n}\left(\frac{Q}{\pi}\right)^{n-1}\left[\left(\frac{1}{n}+3\right)\right]^{n}\left(\frac{d^{-3n}-D^{-3n}}{d^{-3}-D^{-3}}\right). \qquad (4.1)$$

Here λ and n are obtained from the Carreau-Yasuda model, equation (3.1). This relation is only valid in the shear-thinning regime when the shear rate is larger than the critical shear rate ($1/\lambda$) and the viscosity is thus well approximated by $\eta(\dot{\gamma}) \approx \eta_0(\lambda\dot{\gamma})^{n-1}$. For our truncated cone geometry, the minimum value of the wall shear rate is $\dot{\gamma} = 32Q/\pi D^3 = 0.3\ \mathrm{s}^{-1}$, which justifies the use of the power law fluid and equation (3.1) as an approximation. The pressure drop required for the shear-thinning silk dope is a factor of

500 lower than that associated with a corresponding viscous Newtonian fluid. Thus shear-thinning of the liquid crystalline solution reduces the absolute value of the pressure drop in the spinning canal required to sustain flow rates of ~0.1 nL/s. This shear-thinning may also act synergistically with other proposed mechanisms that allow the spinning of the thread, such as a shear-induced transition to a liquid crystalline phase (Vollrath and Knight 2001), localised slip of the polymer solution on the tube wall (Migler *et al.* 1993), or a subtle form of lubrication, such as a watery surfactant layer (Vollrath and Knight 2001) or an analogue to the sericin coat surrounding fibroin fibres spun by *B. mori* (Kaplan *et al.* 1994).

In contrast to the observations of shear-thinning, the measurements of the transient extensional rheology in the micro-capillary break-up extensional rheometer (or μCABER) show that in an elongational flow the material's resistance to stretching increases with elapsed time (and imposed strain). The importance of this strain-hardening phenomena for the spinning of dragline silk appears to have been first noted by Ferguson & Walters (1988) and prevents the capillary break-up of an elongating viscoelastic fluid filament (Olagunju 1999).

In addition to being sheared, the proteins in the spinning dope are also stretched due to the elongational flow experienced in the converging duct and the subsequent spinline. An extensional flow of this type is characterized by the deformation rate and the total Hencky strain accumulated, which can be defined in the present problem as $\varepsilon = 2\ln(D/d) \approx 8$ (Bird *et al.* 1987). This large value of the extensional strain suggests that the spidroin molecules are being considerably extended (Perkins *et al.* 1997). This extension thus plays a key role

in the molecular alignment necessary for the exceptional mechanical properties of the spun fibre. The characteristic strain rate for this elongational flow is given by $\dot{\varepsilon} \approx \frac{4Q}{\pi L}\left(\frac{1}{d^2} - \frac{1}{D^2}\right) = 1 s^{-1}$. This rate of stretching can be compared with the liquid relaxation time via the Deborah number (Bird *et al.* 1987) defined as $De = \lambda \dot{\varepsilon}$, which provides a dimensionless measure of the importance of viscoelastic properties. The computed value of $De \approx 0.5$ indicates that viscoelastic effects should result in modest strain hardening of the dope (i.e. an increase in the resistance to stretching with increasing strain) (Bird *et al.* 1987). This strain-hardening effect is due to chain-stretching of the entangled spidroin macromolecules and the presence of this additional elastic stress can be evaluated from the extensional viscosity of the liquid.

The time evolution in the neck radius that is depicted in figure 3*a* is driven by the capillary pressure and resisted by the viscoelastic stresses in the elongating fluid thread. The necking rate is further modulated by evaporation of solvent (water) from the thread. This evaporation rate becomes larger as time proceeds due to the increasing surface area-to-volume ratio. The loss of water also results in an increase in the fluid viscosity and a further slow down in the rate of necking. A simple model which captures the essential physics of this filament thinning/drying process through a time-dependent viscosity function is given by Tripathi *et al.* (2000). In this analysis, a 'lumped parameter' model is developed which describes the rate of mass transfer in terms of a single dimensionless group referred to as a processability parameter *P*. This parameter is defined as the ratio of the two relevant time scales in the problem: the time scale for capillary thinning and the

time scale for diffusion of water through the viscous protein dope to the free surface. The characteristic time for capillary thinning is $t_{cap} \sim \eta_0 R_0 / \sigma$ (for a viscous fluid) and the time scale for diffusion (which in our case limits water removal from the thread (Kojic *et al.* 2004)) is $t_{diff} \sim {R_0}^2 / D_w$, where R_0 and D_w are the initial thread radius and the diffusivity of water through the dope, respectively. We have recently reported a value $D_w = 2 \times 10^{-5}$ mm^2/s for the diffusivity of water through the *Nephila* spinning dope (Kojic *et al.* 2004). Using this value along with an initial radius of R_0 = 78 microns (see figure 3*a*) we obtain the following estimate of the processability parameter:

$$P \approx \frac{D_w \eta_0}{R_0 \sigma} = 1.6 \times 10^{-2}. \tag{4.2}$$

The analysis of Tripathi *et al.* (2000) utilizes the parameter P to yield a time-varying fluid viscosity given by

$$\eta(t) = \eta_0 \exp\left(2P \int_0^t \frac{R_0}{R(t)} dt \right). \tag{4.3}$$

Combining this time-dependent viscosity with equation (2.1) results in an integro-differential equation for calculating the evolution of the radius of the thinning thread.

Alternatively, it is possible to apply this theory directly to the present microcapillary break-up measurements treating P as an arbitrary fitting parameter. The results of using a best fit value of $P = 2.715 \times 10^{-2}$ are shown in figure 3*a* by the solid line. This best fit value of the processability parameter is in good agreement with the *a priori* estimate given above.

The resistance of the fluid thread to further stretching is characterized by the apparent extensional viscosity (derived from equations (2.1) and (4.3)) as presented in figure 3*b* over the entire course of the filament evolution. At large strains the filament undergoes strain-hardening due to the combined action of molecular elongation and solvent evaporation, and ultimately becomes a solid thread with a constant diameter. The extensional viscosity increases by 100-fold during the capillary thinning of the filament radius. This strain-hardening plays an important role in the fibre spinning process by inhibiting capillary thread break-up and stabilizing the spinline.

Conclusions

In this work we have used two new micro-rheometric devices that utilize less than 5 µl of fluid for a test and enable the measurement of the steady and transient rheological properties of *ex vivo* samples of biopolymer solutions such as spider and silkworm spinning dope. The devices are able to impose large deformation rates and large strains which match the range of deformations experienced *in vivo.* Our measurements show that the steady shear viscosities $\eta(\dot{\gamma})$ of *N. clavipes* and *B. mori* spinning solutions have very large zero-shear-rate viscosities but shear-thin dramatically above a critical deformation rate (see table 1). By contrast, in extensional flow, the apparent extensional viscosity of the spider silk dope increases without bound due to the combined action of molecular elongation and solvent evaporation.

Orb-weaving spiders have evolved a specialized fibre-spinning process that exploits the nonlinear rheology of a complex fluid. In the spinning canal of *Nephila clavipes*, the

shear viscosity of the spinning dope decreases by an order of magnitude in order to reduce the pressure-drop in the canal, whereas the extensional viscosity increases by a factor of one hundred to stabilise the fluid thread and inhibit capillary break-up of the spun thread. Tailoring the rheological properties of artificial spinning dopes containing genetically modified or reconstituted silks to match the *ex vivo* properties of the natural dope may prove essential in enabling us to successfully process novel synthetic materials with mechanical properties comparable to, or better than, those of natural spider silk.

Acknowledgements: This research was supported by funds from the NASA Biologically-Inspired Technology Program, the DuPont-MIT Alliance and in part by the U.S. Army through the Institute for Soldier Nanotechnologies, under Contract DAAD-19-02-D0002 with the U.S. Army Research Office. Adult female *Nephila clavipes* spiders were kindly provided by Rachel Rogers of the Miami MetroZoo.

References

Adamson, A. W. & Gast, A. P. 1997 *Physical Chemistry of Surfaces 6th ed.* New York: Wiley-Interscience.

Bazilevsky, A. V., Entov, V. M. & Rozhkov, A. N. 1990 Liquid Filament Microrheometer and Some of its Applications. In *Third European Rheology Conference* (ed. D. R. Oliver), pp. 41-43. Elsevier Applied Science.

Becker, N., Oroudjev, E., Mutz, S., Cleveland, J. P., Hansma, P. K., Hayashi, C. Y., Makarov, D. E. & Hansma, H. G. 2003 Molecular nanosprings in spider capture-silk threads. *Nat Mater* 2, 278-283.

Bhattacharjee, P. K., Oberhauser, J. P., McKinley, G. H., Leal, L. G. & Sridhar, T. 2002 Extensional Rheometry of Entangled Solutions. *Macromolecules* 25, 10131-10148.

Bird, R. B., Armstrong, R. C. & Hassager, O. 1987 *Dynamics of Polymeric Liquids. Volume 1: Fluid Mechanics*. New York: Wiley Interscience.

Chen, X., Knight, D. P. & Vollrath, F. 2002 Rheological characterization of nephila spidroin solution. *Biomacromolecules* 3, 644-648.

Christanti, Y. & Walker, L. M. 2001 Surface tension driven jet break up of strain hardening polymer solutions. *Journal of Non-Newtonian Fluid Mechanics* 100, 9-26.

Clasen, C. & McKinley, G. H. 2004 Gap-dependent Microrheometry of Complex Liquids. *Journal of Non-Newtonian Fluid Mechanics* 124, 1-10.

Clasen, C. & McKinley, G. H. 2005 submitted Microrheology - The Flexure-based Microgap Rheometer (FMR). *Journal of Rheology*.

Cooper-White, J. J., Fagan, J. E., Tirtaatmadja, V., Lester, D. R. & Boger, D. V. 2002 Drop formation dynamics of constant low-viscosity, elastic fluids. *Journal of Non-Newtonian Fluid Mechanics* 106, 29-59.

Ferguson, J. & Walters, K. 1988 Of Spiders and Spinning. *Chemistry in Britain*, 39-42.

Gearing, B. P. & Anand, L. 2001 A novel testing apparatus for tribological studies at the small scale. *Proc. 2001 ASME Int. Mech. Eng. Congress and Exposition*.

Gosline, J. M., Guerette, P. A., Ortlepp, C. S. & Savage, K. N. 1999 The Mechanical Design of Spider Silks: From Fibroin Sequence to Mechanical Function. *J. Experimental. Biology* 202, 3295-3303.

Jin, H. J. & Kaplan, D. L. 2003 Mechanism of silk processing in insects and spiders. *Nature* 424, 1057-1061.

Kaplan, D., Adams, W. W., Farmer, B. & Viney, C. 1994 *Silk Polymers: Materials Science and Biotechnology*. Washington DC: ACS.

Knight, D. P. & Vollrath, F. 1999 Liquid Crystals and Flow Elongation in a Spider's Silk Production Line. *Proc. Roy. Soc. B* 266, 519-523.

Kojic, N., Kojic, M., Gudlavalleti, S. & McKinley, G. H. 2004 Solvent Removal during Synthetic and Nephila Fiber Spinning. *Biomacromolecules* 5, 1698-1707.

Lazaris, A., Arcidiacono, S., Huang, Y., Zhou, J. F., Duguay, F., Chretien, N., Welsh, E. A., Soares, J. W. & Karatzas, C. N. 2002 Spider silk fibers spun from soluble recombinant silk produced in mammalian cells. *Science* 295, 472-476.

McKinley, G. H. & Tripathi, A. 2000 How to Extract the Newtonian Viscosity from Capillary Breakup Measurements in a Filament Rheometer. *J. Rheol.* 44, 653-671.

Migler, K. B., Hervet, H. & Leger, L. 1993 Slip transition of a polymer melt under shear stress. *Physical Review Letters* 70, 287-290.

Mukhopadhyay, A. & Granick, S. L. 2001 Micro and Nanorheology. *Curr. Opin. Coll. & Int. Sci* 6, 423-429.

Olagunju, D. O. 1999 A 1-D Theory for Extensional Deformation of a Viscoelastic Filament Under Exponential Stretching. *J. Non-Newt. Fluid Mech.* 87, 27-46.

Perez-Rigueiro, J., Elices, M., Plaza, J., Real, J. I. & Guinea, G. V. 2005 The effect of spinning forces on spider silk properties. *Journal of Expiremental Biology* 208, 2633-2639.

Perkins, T. T., Smith, D. E. & Chu, S. 1997 Single Polymer Dynamics in an Elongational Flow. *Science* 276, 2016-2021.

Shao, Z. & Vollrath, F. 2002 Surprising strength of silkworm silk. *Nature* 418, 741.

Solomon, M. & Lu, Q. 2001 Rheology and Dynamics of Particles in Viscoelastic Media. *Curr.. Opin. Colloid & Int. Sci.* 6, 430-437.

Terry, A. E., Knight, D. P., Porter, D. & Vollrath, F. 2004 pH induced changes in the rheology of silk fibroin solution from the middle division of Bombyx mori silkworm. *Biomacromolecules* 5, 768-772.

Tripathi, A., Whittingstall, P. & McKinley, G. H. 2000 Using filament stretching rheometry to predict strand formation and "processability" in adhesives and other non-Newtonian fluids. *Rheologica Acta* 39, 321-337.

Trouton, F. T. 1906 On the Coefficient of Viscous Traction and its Relation to that of Viscosity. *Proc. R. Soc. Lond.* A77, 426-440.

Vollrath, F. & Knight, D. P. 2001 Liquid crystalline spinning of spider silk. *Nature* 410, 541-548.

Willcox, P. J., Gido, S. P., Muller, W. & Kaplan, D. L. 1996 Evidence of a Cholesteric Liquid Crystalline Phase in Natural Silk-Spinning Processes. *Macromolecules* 29, 5106-5110.

Yasuda, K., Armstrong, R. C. & Cohen, R. E. 1981 Shear-flow properties of concentrated-solutions of linear and star branched polystyrenes. *Rheologica Acta* 20, 163-178.

Table 1. Constitutive parameters for the shear viscosity of *B. mori* and *N. clavipes* spinning dope. Zero shear viscosity η_0, relaxation time λ, power-law index n and transition parameter a of the Carreau-Yasuda equation (3.1).

Figure 1: a, Adult female *Nephila Clavipes* (golden-orb) spider provided by the Miami Metrozoo, Florida. Scale bar is 2cm. **b,** (A) Dissected major ampullate (MA) gland of the spider (scale bar 1 mm). The ~1 μL blob (B) protruding through a rupture of the gland wall near the spinning canal (C) was used for the rheology experiments.

Figure 2: a, Schematic diagram of the flexure-based micro-rheometer. The fluid sample is sheared between two interferometrically-aligned flat plates (A). The compound flexure system (B) is actuated by an "inchworm" motor (C) and provides a planar (Couette) shear flow. The shear stress is deduced from the corresponding deflection of the top fixture as detected by an inductive sensor (D). **b,** Shear viscosity of the native silk dope. Diamonds (and shaded red area) correspond to *Nephila clavipes* spider; open circles (and blue shaded area) are from *Bombyx mori* silkworm. The solid lines (blue for silkworm and red for spider) represent the Carreau-Yasuda fit from equation (3.1) to experimental data (markers). Reproducibility was confirmed by testing specimens from two other spiders and silkworms whose abdomens were similar in size. The variation in the data is represented by the shaded band.

Figure 3: a, Radius of necking thread formed from the *ex vivo* obtained *Nephila* dope (measured at thread midpoint, see inset in panel *b*) in red markers. The solid black line represents the model fit using the processability parameter of $P = 2.715\times10^{-2}$. **b,** The transient extensional rheology of *ex vivo* spider dope. The extensional viscosity is shown as a function of the total strain in the material. Here, R_0 is the initial diameter of the thread measured at the midpoint between the plates with a laser micrometer. The decrease of the midpoint radius was monitored over time (see panel *a*). The extensional viscosity was then deduced from equation (2.1) and is represented by the markers. The solid line is an analytical fit of these values. For low strains, we obtain the limit $\eta_e \approx 3\eta_0 = 11400$ Pa.s as expected for a Newtonian liquid. Inset, a silk thread of diameter 40 μm formed by separating the plates to a distance of 5 mm and allowing the thread to neck under the action of capillarity and viscoelastic stresses (scale bar is 1mm).

Table 1. Constitutive parameters for the shear viscosity of *B. mori* and *N. clavipes* spinning dope. Zero shear viscosity η_0, relaxation time λ, power-law index n and transition parameter a of the Carreau-Yasuda equation (3.1).

	η_0 (Pa.s)	λ (s)	n	a
Bombyx mori	5200	0.57	0.17	0.80
Nephila clavipes	3500	0.40	0.18	0.68

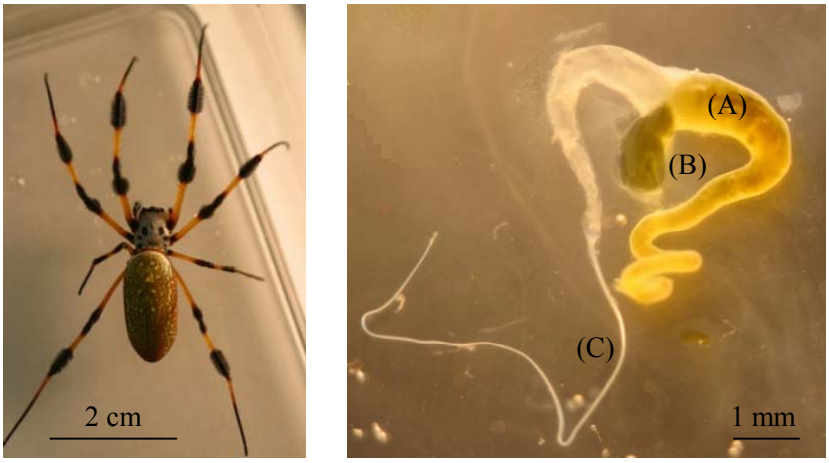

a **b**

Figure 1: a, Adult female *Nephila Clavipes* (golden-orb) spider provided by the Miami Metrozoo, Florida. Scale bar is 2cm. **b,** (A) Dissected major ampullate (MA) gland of the spider (scale bar 1 mm). The ~1 μL blob (B) protruding through a rupture of the gland wall near the spinning canal (C) was used for the rheology experiments.

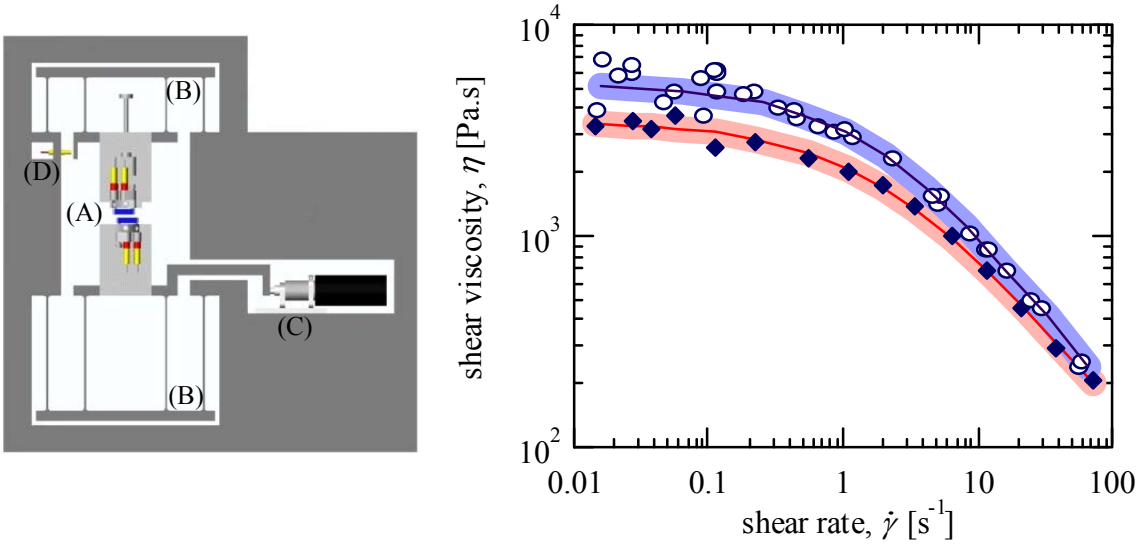

a **b**

Figure 2: a, Schematic diagram of the flexure-based micro-rheometer. The fluid sample is sheared between two interferometrically-aligned flat plates (A). The compound flexure system (B) is actuated by an "inchworm" motor (C) and provides a planar (Couette) shear flow. The shear stress is deduced from the corresponding deflection of the top fixture as detected by an inductive sensor (D). **b,** Shear viscosity of the native silk dope. Diamonds (and shaded red area) correspond to *Nephila clavipes* spider; open circles (and blue shaded area) are from *Bombyx mori* silkworm. The solid lines (blue for silkworm and red for spider) represent the Carreau-Yasuda fit from equation (3.1) to experimental data (markers). Reproducibility was confirmed by testing specimens from two other spiders and silkworms whose abdomens were similar in size. The variation in the data is represented by the shaded band.

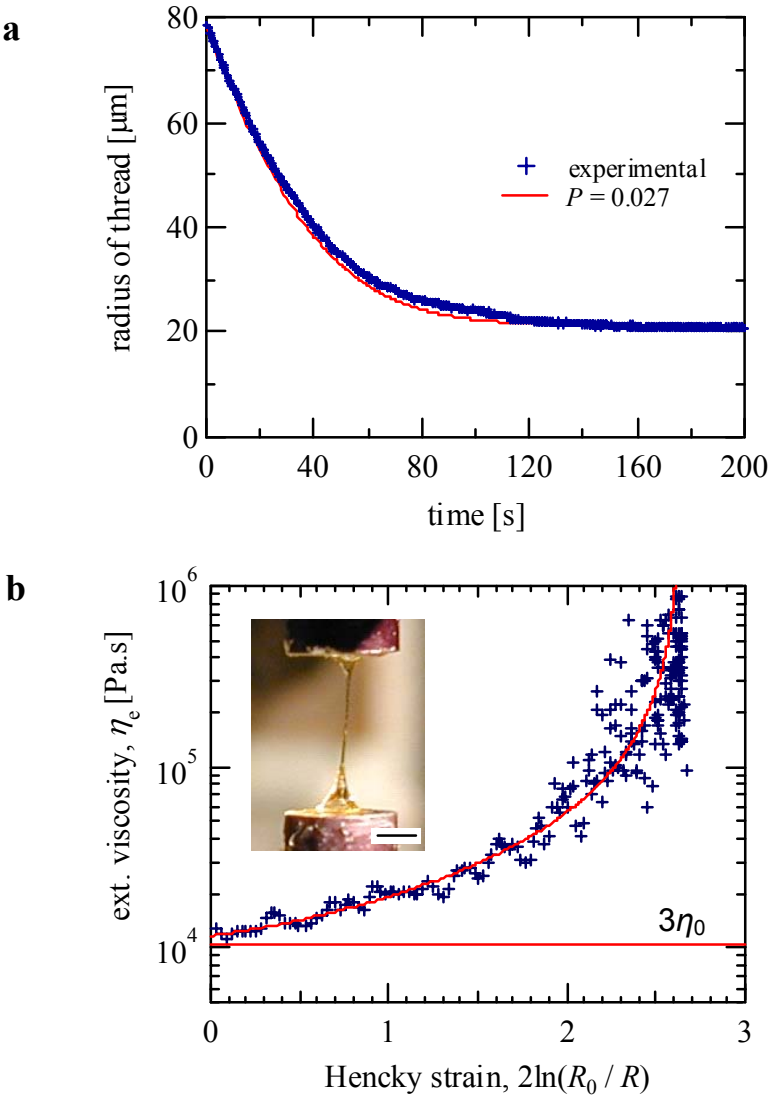

Figure 3: a, Radius of necking thread formed from the *ex vivo* obtained *Nephila* dope (measured at thread midpoint, see inset in panel *b*) in red markers. The solid black line represents the model fit using the processability parameter of $P = 2.715\times10^{-2}$. **b,** The transient extensional rheology of *ex vivo* spider dope. The extensional viscosity is shown as

a function of the total strain in the material. Here, R_0 is the initial diameter of the thread measured at the midpoint between the plates with a laser micrometer. The decrease of the midpoint radius was monitored over time (see panel *a*). The extensional viscosity was then deduced from equation (2.1) and is represented by the markers. The solid line is an analytical fit of these values. For low strains, we obtain the limit $\eta_e \approx 3\eta_0 = 11400$ Pa.s as expected for a Newtonian liquid. Inset, a silk thread of diameter 40 μm formed by separating the plates to a distance of 5 mm and allowing the thread to neck under the action of capillarity and viscoelastic stresses (scale bar is 1mm).